INVESTIGATIVE NUCLEAR MEDICINE

Basal Kinetic Studies of Tc-99m DMPE as a Myocardial Imaging Agent in the Dog

Hiroshi Nishiyama, Edward Deutsch, Robert J. Adolph, Vincent J. Sodd, Karen Libson, Eugene L. Saenger, Myron C. Gerson, Marjorie Gabel, Steven J. Lukes, Jean-Luc Vanderheyden, Donald L. Fortman, Kenneth L. Scholz, Laurence W. Grossman, and Craig C. Williams

University of Cincinnati and Bureau of Radiological Health, Cincinnati, Ohio

Newly synthesized Tc-99m dichlorobis(1,2-dimethylphosphino)ethane (DMPE) was investigated as a myocardial imaging agent with respect to its kinetics (dependent on both time and on regional coronary blood flow), its percent organ uptake, and its imaging characteristics in the anesthetized dog. Most of these data are compared with those of Tl-201. Blood clearance of the two agents is essentially the same. Compared with Tl-201, Tc-99m DMPE shows faster overall kinetics, higher heart-to-lung ratio, equally good correlation with a wide range of regional blood flows, and higher liver uptake. At the time of peak myocardial uptake, the mean heart uptake of Tl-201 is 4.3%, compared with 2.9% for Tc-99m DMPE, yet only 0.9% uptake of Tc-99m DMPE is found in the lung as compared with 3.3% for Tl-201. These differences result in a heart-to-lung ratio of 2:1 for Tc-99m DMPE and 1:1 for Tl-201, based on the data obtained from the time-activity curve. The quantitative findings are supported by the superior quality of Tc-99m DMPE images of both normal and infarcted dog heart. The high hepatic uptake of Tc-99m DMPE is not a serious problem if images are obtained within 5–60 min after dose. These basic kinetic studies suggest that Tc-99m DMPE is a promising myocardial imaging agent.

J Nucl Med 23: 1093–1101, 1982

The early results of our continuing search for Tc-99m labeled myocardial imaging agents have been detailed (*1*). This work led to a series of agents, the Tc-99m *o*-phenylene-bis(dimethylarsine) (DIARS) compounds, which successfully imaged the dog myocardium, but were not soluble in water. More recently we have developed the water soluble compound, *trans*-dichlorobis[Tc-99m (III) DMPE], where DMPE = bis(1,2-dimethylphosphino)ethane, hereafter referred to as Tc-99m DMPE. The chemical properties, structure and preliminary description of Tc-99m DMPE in the dog myocardium have been reported recently (*2*). The development of Tc-99m DMPE has resulted from a program aimed at generating monocationic Tc-99m complexes of known chemical structure, this structure being established by classical chemical techniques applied to the analogous Tc-99m complex (*2*).

The purpose of this communication is to report properties of Tc-99m DMPE as a myocardial imaging agent based on an experimental animal study. We report time-dependent kinetics, percent organ uptake, blood-flow-dependent kinetics and imaging characteristics in anesthetized dogs in the resting state. These basic kinetic and imaging data are compared with those of Tl-201, some of which were reported previously using a similar experimental design (*3*).

Received Mar. 19, 1982; revision accepted July 12, 1982.

For reprints contact: H. Nishiyama, MD, Nucl. Med. Lab., DEP, BRH, FDA, Cincinnati General Hosp., Cincinnati, OH 45267.

MATERIALS AND METHODS

Tc-99m DMPE. The preparation and chemistry of this agent have been detailed in a recent report from our

institution (*2*). This preparation employs $^{99m}TcO_4^-$ from a Mo-99/Tc-99m generator, excess DMPE ligand to reduce $^{99m}TcO_4^-$ and stabilize the technetium(III) product, HCl to keep the pH of the reaction medium *ca.* 2, an ethanol/water reaction medium to maintain all species in homogeneous solution, and high temperature to drive the reaction to completion. Each preparation was analyzed before use by reversed-phase, high-performance liquid chromatography to assess its radiochemical purity. The typical Tc-99m DMPE purity was over 95%, but occasionally it fell as low as 87%; all preparations were used directly, no attempt being made to separate the major Tc-99m DMPE component from the minor amounts of impurities.

Time-dependency. This study of time-dependency consisted of two parts: (a) time-activity curves obtained over the heart, lung, and liver to evaluate the changing heart-to-nontarget ratios; and (b) blood clearance. Six normal mongrel dogs weighing 26–35 kg were studied. Each dog was anesthetized and placed under a gamma camera with a high-resolution collimator in the 60° left anterior oblique view. Five to seven mCi (185–259 MBq) of Tc-99m DMPE were given intravenously as a bolus. The beginning of the intravenous administration was designated as time zero, and data were stored continuously in a computer in one-min frames for the first 30 min. Thereafter, data were obtained every 10–20 min in two consecutive one-min frames until 120 min after dose. Time-activity curves were generated from the stored data by defining the region of interest over the myocardial wall and the backgrounds over the lung and liver. The digital image of the initial one-min blood-pool phase was used to define the lung background in the area located between the aorta and ventricular cavity (*3*). Digital images acquired after the blood-pool image were used to designate the region of interest over the anterior myocardial wall and the liver background, which was selected as an area at the upper edge of the liver. The lung background was subtracted from the count of the anterior wall at each data point and the maximum net count was considered to be 100%. The remainder of the net counts at each data point, including the background, were expressed relative to this 100% value of the anterior wall. Polaroid images were obtained at frequent intervals.

For the withdrawal of blood samples, in the first four dogs an indwelling catheter was fed into the superior vena cava through a jugular vein, and the total activity administered was measured with a calibrated Ge(Li) detector. Each blood sample was weighed, counted in a well counter, and corrected for decay to the time of withdrawal. Finally, the sample was expressed as activity per ml using the conversion [one gram would occupy 1/1.06 ml] factor of 1.06 from cpm/g to cpm/ml (*4*). Known activity administered at time zero was considered as 100% activity, based on the assumption that an even distribution of the agent had occurred throughout the blood, whose volume was later measured with Cr-51-labeled red blood cells and I-125-labeled human serum albumin.

Organ uptake. Two normal dogs, weighing 26 and 27 kg, were anesthetized and the chest opened. A catheter was introduced into the left atrium for subsequent administration of microspheres, and the chest closed. For the dual-tracer study of organ uptake, it was important to collect samples at the times of maximum heart uptake. Accordingly, referring to the time-activity curves, Tl-201 was injected i.v. at 40 min before sacrifice (*3*), and Tc-99m DMPE only 15 min before. Then, at 5 min before sacrifice, a flow marker of Sr-85 microspheres (8 to 10 million particles, 10 μm diam) was delivered into the left atrium through the catheter. Homogeneous distribution of the microspheres was assured by at least 5 min in a vortex mixer just before injection, and they were delivered slowly to avoid disturbing cardiac function. The dog was then killed, and the heart removed and freed from the roots of the great vessels and excess fat. It was counted in the whole-body counter room, with a 20- by 10-cm NaI(Tl) detector and 4000-channel analyzer. On the basis of a phantom study, to be described immediately, the uptakes in the heart, lungs, liver, spleen, and kidneys were calculated as percentages of administered activity.

The organ phantom, a 400-ml plastic container, was filled with water to approximately the volume of each organ to be counted. Known activities of Tc-99m, Tl-201, and Sr-85, measured with a Ge(Li) detector, were placed in the water and counted for 3 min. After background subtraction and correction of Compton scatter, the calibration factors (cpm/mCi or cpm/37 MBq) were determined for each radionuclide. Whole organs were placed in the 400-ml container and counted under similar conditions. The liver was weighed and a known fraction counted. The net counts in each organ were decay-corrected to the time of radionuclide administration, and the activity was calculated using the calibration factor. This was then expressed as the percent of the known administered dose.

The organ uptake study was carried out on two dogs with normal hearts. Two others, of similar weight, were anesthetized and the chest opened. To induce an acute myocardial infarct, the circumflex coronary artery was totally occluded for 45 min, then released. The chest was then closed (*5*). Organ uptakes were determined in these dogs as in the normal ones.

Flow-dependency. The flow-dependency study was to determine the relationship between coronary blood flow and uptake of both Tc-99m DMPE and Tl-201. After measurement of the percent organ uptake in each of the four hearts described above, the right ventricular wall and atria were removed. After removal of the apex en bloc, five nearly equal cross sections of the left ventricle

were made by slicing from the apex to the base. Each segment exclusive of the apex was divided into eight nearly equal transmural blocks, each of which was further subdivided into endocardial and epicardial halves. The apex was divided into four longitudinal samples. The 84 samples from each heart (5 segments × 8 blocks × 2 transmural halves + 4 apical samples) were then counted for Tc-99m, Tl-201, and Sr-85 in the well counter equipped with a 2,000-channel analyzer. After appropriate correction for background and Compton scatter, the counts obtained from each radionuclide were corrected for decay to the time of death, and the final count was expressed per gram of tissue. For each radionuclide, the three samples with the highest counts per g in each heart were averaged and designated as 100%. The percent counts in the other samples were normalized to these 100% values for each of the three radionuclides. Then, a linear regression analysis was applied to the flow marker and two myocardial imaging agents.

Imaging. Five mongrel dogs weighing 25–31 kg were prepared by induction of an acute myocardial infarct (*5*). Images were obtained in the anterior, 45° left anterior oblique, and left lateral views on three occasions in each dog; first with Tl-201 and then with Tc-99m DMPE, collecting total counts of 500K per view. Activities used were 5–7 mCi (185–259 MBq) for Tc-99m DMPE and about 2 mCi (74 MBq) for Tl-201, administered intravenously. The optimal imaging time for Tc-99m DMPE was determined from the time-dependency study described above. The optimal imaging time for Tl-201 calls for starting at 20–25 min after administration, as previously reported (*3*). Upon completion of the third imaging study, the dog was killed with an overdose of pentobarbital and the heart was removed. It was sliced horizontally, parallel to the base, into six segments, and stained with triphenyl tetrazolium chloride (TTC) for identification of the infarct (*6*). These stained segments were then compared with the previously obtained scintigrams.

RESULTS

Blood clearance. Figure 1 shows the average blood clearance through 40 min after dose, based on four dogs for Tc-99m DMPE and on three for Tl-201 (*3*). The remaining mean percent activities in the blood pool for Tc-99m DMPE and Tl-201, respectively, were: at 1 min after dose 32.4 (range: 27.0–37.0) and 23.9 (20.5–27.2); at 5 min 5.3 (5.0–5.8) and 8.1 (5.9–11.4); at 20 min 3.0 (2.7–3.3) and 2.4 (2.2–2.7); and at 120 min 1.8 (1.5–2.0) and 1.4 (1.4–1.6). Although these data suggest a somewhat faster blood clearance for Tl-201, the rates for the two agents can be considered essentially the same.

Time-activity curves. These curves are shown in Fig. 2. Because the image characteristics were defined as a function of real time, the time-activity curves are not

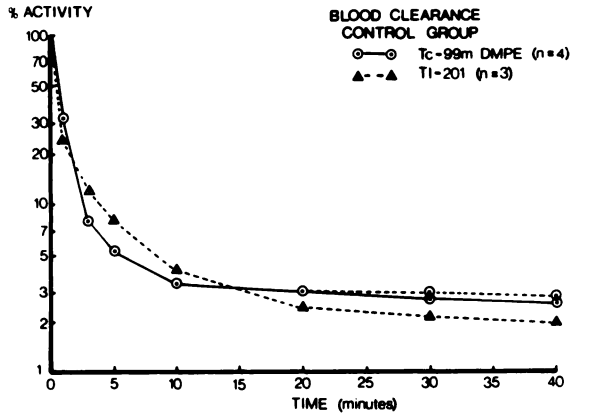

FIG. 1. Blood clearance of Tc-99m DMPE and Tl-201 (semilog). (- - ⊙ - -) indicates values after Tc-99m decay correction.

decay-corrected. If the Tc-99m activity were decay-corrected, the mean Tc-99m DMPE would be 60.8% at 120 min, compared with the uncorrected value of 49.0%. The peak myocardial uptake of Tc-99m DMPE was observed at 15 min after dose. Similar data for Tl-201 obtained under the same conditions are also shown in Fig. 2. The maximum uptake was observed 40 min after dose, and 90.3% of the maximum remained at 120 min (*3*). The salient difference between the two agents is the substantially faster kinetics of Tc-99m DMPE.

The lung background is considered to have a major effect upon the image quality. Figure 3 shows the time-activity curves of Tc-99m DMPE observed in the anterior myocardial wall, lung, and liver. At the time of maximal myocardial uptake, the lung background is about half of the myocardial activity and the target-to-nontarget ratios thereafter remain approximately 2:1. On the other hand, the liver background increases rapidly to a level approximately three times that of the myocardium at 10–15 min after dose, followed by a slow washout. In fact, when the Tc-99m counts in the liver background are decay-corrected, the mean liver background becomes almost constant beginning about 80 min after dose.

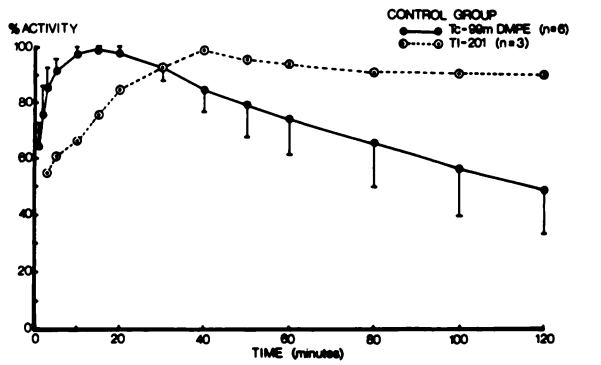

FIG. 2. Time-activity curves of Tc-99m DMPE (mean ± s.d.) and Tl-201 (mean) in normal myocardium are compared. Note faster kinetics of Tc-99m DMPE. No correction for decay is included.

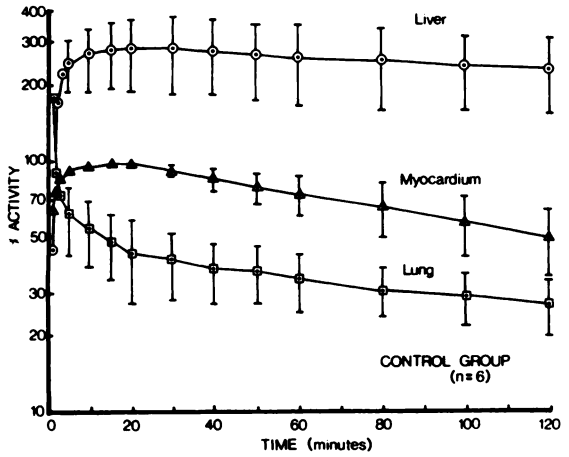

FIG. 3. Lung and liver backgrounds obtained from Tc-99m DMPE study are shown in relation to myocardial activity (semilog, mean ± s.d.). On average, activity in liver over a unit area is about three times the activity in myocardium. Low lung background leads to target-to-nontarget ratios of about 2:1.

Although the liver uptake of Tc-99m DMPE is high, this detracted little from the image quality, presumably because of the excellent target-to-nontarget ratio. Thallium-201 also shows activity in the liver, but not to the degree observed with Tc-99m DMPE. The relationship between lung background and myocardial activity in these two agents is shown in Fig. 4. The heart-to-lung ratios for Tl-201 remain approximately 1:1 beginning 40 min after dose, when the maximal myocardial uptake of Tl-201 is observed (*3*). The heart-to-lung ratios found in this study agreed with the Tl-201 values found by other investigators (*7,8*). These relationships are reflected in the myocardial images obtained at various time intervals, shown in Fig. 5. We conclude that the optimal imaging time for Tc-99m DMPE is ~10–40 min after dose, but satisfactory images are consistently obtained as early as 5 min and as late as 60 min after dose.

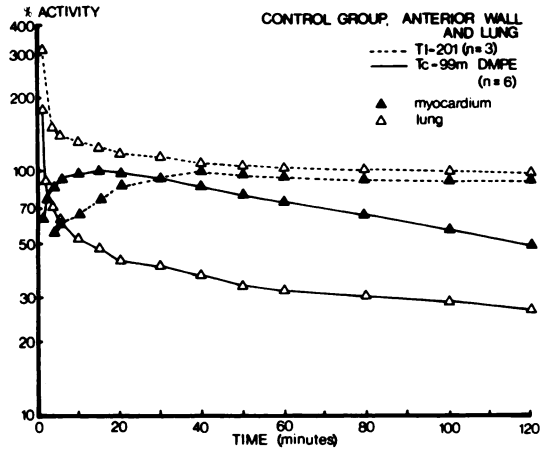

FIG. 4. Target-to-nontarget ratios computed on mean values for Tc-99m DMPE and Tl-201, are compared. With Tl-201, T/NT remains at ~1, following its peak myocardial concentration at 40 min after dose.

Effective and biological half-times. From the kinetic data, both effective ($t_{1/2}$ eff.) and biological ($t_{1/2}$ biol.) half-times were calculated by fitting the activity curves to the least-squares model, $Y = Ae^{-\tau x}$, where τ is the decay constant and χ is the time after dose. The results are shown in Table 1. These curve fittings were based on data points observed after the time of maximal activity in each organ. The data showed a marked difference in myocardial retention time between two agents. Although the $t_{1/2}$ biol. of Tc-99m DMPE in the liver was infinite based on the limited data points, this did not truly reflect the biological pathway of Tc-99m DMPE, since activity was eventually excreted from the gall bladder to the intestine. It is also excreted by the kidneys, as evidenced by activity in the kidney and urinary bladder.

Percent organ uptake. The percent organ uptakes for the heart and other organs, relative to the maximum myocardial uptake of the respective agent, were examined first in the two normal dogs and then in the two dogs with infarcts. The values in these two groups showed little difference for each organ, including the heart. Accordingly, data obtained from all four dogs were combined and the results are shown in Table 2. At maximal uptake, and on average, Tl-201 concentrates in the heart 50% better than Tc-99m DMPE at maximum, both as fractions of total administered activity. However, Tl-201 shows 3.7 times the lung uptake of Tc-99m DMPE. These data further support the finding of a high target-to-nontarget ratio of Tc-99m DMPE. The mean percent activity of Sr-85 microspheres recovered in the heart is 4.7% (range: 3.1–6.3%) in four dogs. This generally accepted normal value indicates that the myocardial blood flow is not altered during the experiment. The higher percent liver uptake of Tc-99m DMPE is in agreement with the higher liver background.

Flow-dependency. The study of blood-flow dependency was designed to ensure that the maximal myocardial uptakes of the two agents coincided, based on the findings of the time-dependent kinetic study. That is, Tl-201 was administered first, and then 25 min later, Tc-99m DMPE was administered. The dog was then sacrificed 15 min later. In this manner, the requirement that the maximal myocardial uptakes of Tl-201 (40 min after dose) and of Tc-99m DMPE (15 min after dose) coincided. Dogs also received Sr-85 microspheres in order to correlate the regional myocardial blood flow with the regional myocardial distributions of these two agents. Results based on the 168 samples obtained from the two normal hearts showed correlation coefficients (r) for flow vs. uptake of 0.98 for Tc-99m DMPE and 0.97 for Tl-201. Another 168 samples from two infarcted hearts showed r = 0.97 for Tc-99m DMPE and 0.96 for Tl-201. This relationship between regional flow and uptake was

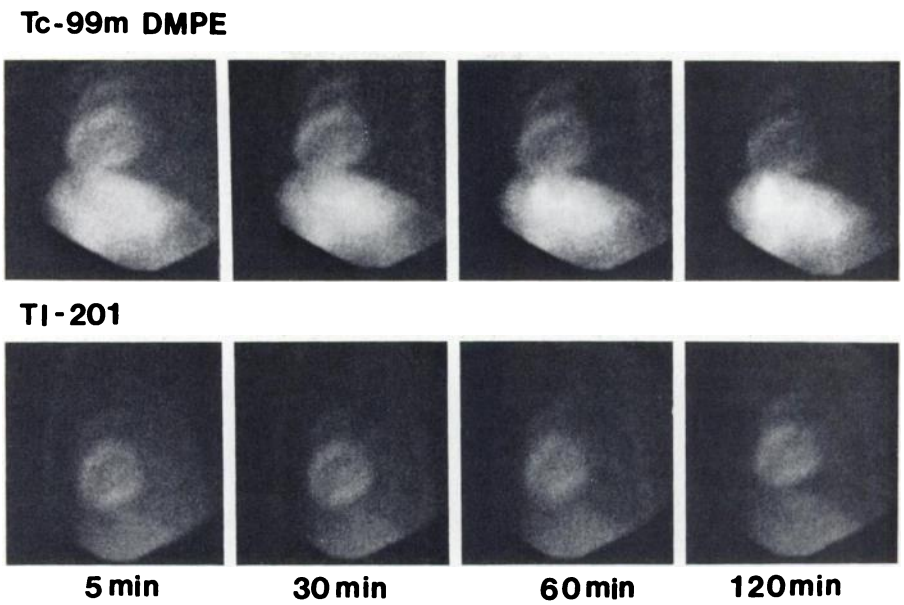

FIG. 5. For Tc-99m DMPE, good-quality images are obtained 5–60 min after dose. Note good definition of myocardial wall, low lung background, but high liver background. Also note increasing activity in dog's biliary system with time. Tl-201 images are shown for comparison. Falling quality of Tc-99m DMPE image with time is due to faster washout from myocardium, but relatively slower washout from lung and liver.

further examined by selecting samples from the infarcted hearts where the blood flow was less than 25% of the maximum. Forty-seven samples met this criterion. The correlation coefficients for these samples were 0.95 for Tc-99m DMPE and 0.91 for Tl-201 (Fig. 6). These results indicate that the regional flow dependency of Tc-99m DMPE uptake at rest is at least as good as that of Tl-201.

Imaging. Five dogs with infarcts were imaged, collecting 500K counts per image, with Tl-201 starting 25–30 min after dose, followed by imaging with Tc-99m DMPE starting at 10 min after dose. The imaging studies were timed in this manner to meet the optimal imaging time for each agent. A clearer definition of the myocardial wall was seen in every Tc-99m DMPE image, compared with Tl-201. Although the liver background was high with Tc-99m DMPE, the diaphragmatic region of the heart was reasonably well separated in most of the projections. Ambiguity in the diaphragmatic region was a problem in some of the projections, but this was usually resolved by other projections. When the liver was poorly defined with Tl-201, the lung background appeared higher in all five dogs studied repeatedly up to 168 hr after infarct. Since all dogs were fasted overnight before each imaging study, the metabolic state of the gastrointestinal system does not appear to be a determining factor.

Figures 7 and 8 show Tc-99m DMPE and Tl-201 images obtained in the infarcted dogs. Figure 9 is a photograph of the slices of one heart stained with triphenyl tetrazolium chloride (*6*). The heart was obtained immediately after imaging study shown in Fig. 8. Although the images in Figs. 7 and 8 demonstrate better defined myocardial wall with Tc-99m DMPE, there is little difference between the two tracers in the definition of the infarcted region. In total, five infarcted dogs were imaged each at three different times after infarct: between 4.5 and 24 hr, at approximately 72 hr, and be-

TABLE 1. EFFECTIVE AND BIOLOGICAL HALF-TIMES (HR)

Organ	Tc-99m DMPE		Tl-201	
	$t_{1/2}$ eff	$t_{1/2}$ biol	$t_{1/2}$ eff	$t_{1/2}$ biol
Myocardium (anterior wall)	1.9	2.8	7.2	8.0
Lung (Bkg-1)	2.6	4.5	6.8	7.5
Liver (Bkg-2)	6.1	*	†	†

* See text for explanation.
† Data were not obtained.

TABLE 2. PERCENT ORGAN UPTAKE IN MONGREL DOGS (n = 4, MEAN AND RANGE)

Organ	Tl-201	Tc-99m DMPE
Heart	4.3 (4.0–4.7)	2.9 (2.2–3.6)
Lung	3.3 (2.0–4.9)	0.9 (0.7–1.0)
Liver	13.6 (11.6–15.6)	21.5 (13.3–33.4)
Spleen	2.3 (0.7–3.1)	1.7 (1.1–2.0)
Kidneys	12.0 (7.5–17.3)	6.5 (3.8–9.4)

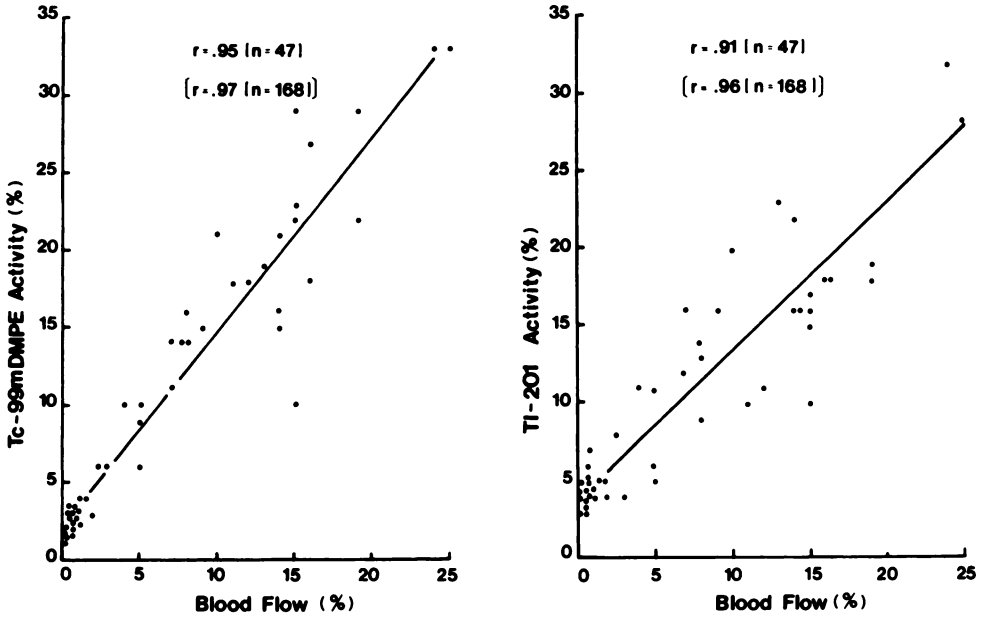

FIG. 6. Relationship between regional activity distribution and blood flow. Figure shows regions with blood flow less than 25% of maximum in 47 samples among a total of 168 samples obtained from two dogs with infarcted hearts. Note better relationship with Tc-99m DMPE, particularly in region with lower blood flow. Correlation coefficients in parentheses are based on all 168 samples obtained from both infarcted dog hearts over 0–100% regional blood-flow range.

tween 144–168 hr. Thus, 15 pairs of images were obtained for evaluation, both with Tl-201 and Tc-99m DMPE. The evaluating scheme was based on how well the images defined the uninvolved myocardium and the infarct. Each pair of images was compared and classified by the consensus of three experienced observers. In 13 of the 15 pairs of images, the Tc-99m DMPE images showed a better-defined myocardial wall, and in the two remaining pairs, the Tc-99m DMPE images were as good as those obtained with Tl-201. In nine out of 15 pairs the infarct was defined better with Tc-99m DMPE; in five pairs the infarct was equally well defined with the two agents, and in one pair the Tl-201 image was superior. None of the observers felt that the high liver back-

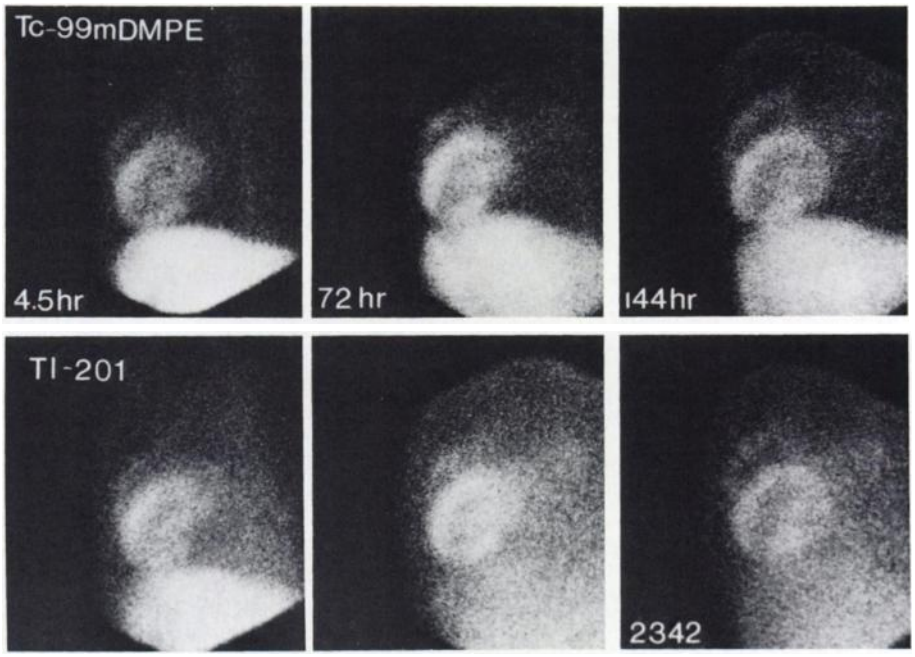

FIG. 7. LAO images from infarcted dog at different times after infarct. With Tc-99m DMPE, generally better defined outline of left-ventricular wall is noted, together with low lung background but high liver background. Definition of infarct at 4.5 and 72 hr after infarct is judged equally good with both agents. At 144 hr after infarct, infarct is judged to be better defined with Tc-99m DMPE.

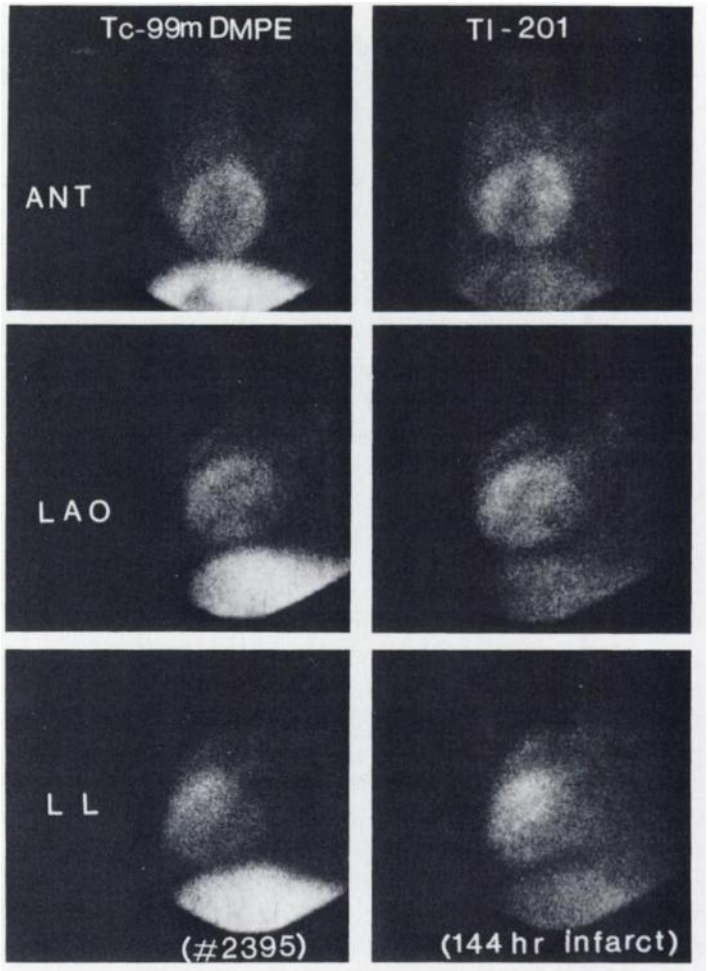

FIG. 8. Large transmural infarct in posteroinferior wall and apical region obtained at 144 hr post-infarct. Both outline of left-ventricular wall and definition of infarct are judged better with Tc-99m DMPE.

ground of Tc-99m DMPE was a serious drawback. No definite difference was noted with respect to image quality and the imaging time after infarct.

DISCUSSION

We have attempted to compare the kinetics of Tc-99m DMPE and Tl-201 in the basal state of the mongrel dogs.

FIG. 9. Heart of dog from Fig. 8, removed immediately after imaging study and stained with TTC. Six segments are shown by looking in a base-to-apex direction. Note large inferior to posterior wall infarct extending into apical region, agreeing well with images shown in Fig. 8.

Blood clearance and time-activity curves are essential to define the imaging properties as a function of time. For example, although the blood clearance rates are essentially the same for Tc-99m DMPE and Tl-201, they do not predict the time after dose of the maximal heart-to-lung uptake ratio, i.e., 15 min after dose for Tc-99m DMPE and 40 min for Tl-201. The percent organ uptake was measured in vitro and the target-to-nontarget ratios so obtained confirm the qualitative differences noted in in-vivo studies. The relationship between regional coronary blood flow and myocardial uptake further clarified the kinetic properties of Tc-99m DMPE, which are clearly dependent on regional flow, as in Tl-201.

Thallium-201 has been widely accepted as the agent of choice for myocardial scintigraphy, based on its myocardial distribution, which is closely proportional to regional myocardial blood flow. In addition, Tl-201 exhibits the unique feature of redistribution following an exercise-induced perfusion defect. However, its shortcomings include high cost and less-than-desirable physical properties as an imaging agent (*9,10*). Many investigators have searched for possible alternatives, such as I-123-labeled heptadecanoic acid (*11*) and/or Te-123m-labeled fatty acids (*12*). These labeled compounds

have at least one similar drawback. The radionuclide must be produced by a cyclotron, and the resulting high cost precludes its wide applicability. Technetium-99m, on the other hand, has desirable physical characteristics and is widely available from a low-cost generator. Thus, Tc-99m DMPE has potential advantages in terms of physical properties, cost, and the possibility of ready, in-house availability.

The kinetics of Tc-99m DMPE are qualitatively similar to those of Tl-201, although the mechanism of Tc-99m DMPE concentration in the myocardium is not known. The known differences between Tc-99m DMPE and Tl-201 are the physical half-life (6 hr vs. 73), molecular weight (399 vs. 201), lipophilicity (Tc-99m DMPE is more lipophilic), and structure (coordination complex vs. hydrated ion). From our earlier work on cationic Tc-99m complexes (*1*), distribution kinetics do not appear to depend primarily on the molecular weight of the complex, and the results with Tc-99m DMPE agree with this generalization. The differences in kinetics among those cations investigated earlier as myocardial imaging agents (*13*) appear also to have little relationship to molecular weight. Our preliminary data indicate that approximately 18% of Tc-99m DMPE is excreted in the urine in 24 hr, compared with 5% for Tl-201 in the dog and about 4% in man (*14*). A high hepatic uptake of Tc-99m DMPE resulted in 25–30% of excretion in the feces in 24 hr, but with Tl-201 this pathway in the human appeared to be insignificant (*14*).

The long $t_{1/2}$ eff. and $t_{1/2}$ biol. of Tc-99m DMPE in the liver raise the question as to whether the hepatocyte or the reticuloendothelial system plays a dominant role in its uptake and excretion. Participation by the reticulo-endothelial system is implied by the observation of Tc-99m DMPE activity in the skeletal system, beginning 30–60 min after dose as the myocardial activity decreases. The outline of the ribs, scapulae, vertebrae, and pelvic bones becomes increasingly clear with time, but the distal portions of the humerus and femur are not visible even after several hours. Thus the distribution of Tc-99m DMPE is reminiscent of that of Tc-99m sulfur colloid. In addition, the uptakes of Tc-99m DMPE in the liver and spleen in Table 2 are in the ratio expected for the function of the reticulo-endothelial system in these two organs. Nevertheless, participation of the hepatocyte system is also implied by the rapid accumulation of Tc-99m DMPE in the gallbladder, and its subsequent discharge into the intestine. This behavior is similar to that observed for the Tc-99m imidodiacetic acid complexes, except that the biological half-life of Tc-99m DMPE is much longer (*15,16*). It thus appears reasonable to assume that Tc-99m DMPE in vivo consists of both colloidal and noncolloidal forms. However, the colloidal forms are probably produced in vivo since all our preparations were passed through a 0.22 μm Millipore filter, and a typical Tc-99m DMPE preparation examined by laser scattering showed no detectable colloids in the range 1–200 nm*. We note that in vivo production of colloids does not imply that Tc-99m DMPE is chemically unstable. In fact, HPLC analysis shows that the millimolar solutions of Tc-99m DMPE in 0.2 *M* aqueous NaCl undergo no detectable hydrolysis or decomposition over a period of 3 wk.

The Tc-99m DMPE concentration in the liver (per unit area) is, on the average, three times that in the myocardium, and this is not a desirable feature for a myocardial imaging agent. However, the clearer definition of the myocardial wall in Tc-99m DMPE images, compared with that in Tl-201 images, appears to compensate for this potential drawback. Partially shielding the liver in order to increase the contrast with the myocardium did not noticeably improve the image quality in our experience. However, this practice could be important when gated or single-photon emission computed tomography studies are conducted. Currently we are modifying the Tc-99m DMPE synthetic procedure in the hope of reducing hepatic uptake, which would enhance the relative myocardial uptake.

The absolute concentration of Tc-99m DMPE in the myocardium is lower than that of Tl-201, but the far lower concentration of Tc-99m DMPE in the lung results in a superior target-to-nontarget ratio and hence better-quality images. Furthermore, the equally good correlation between the regional myocardial blood flow and Tc-99m DMPE concentration could likely provide an additional advantage and may result in better definition of ischemic regions. Early evaluation of patients with possible acute myocardial infarction is important, since early intervention may limit infarct size. Thus, the ready availability of an in-house preparation would be desirable. If the Tc-99m DMPE proves useful, a kit form is quite feasible.

Our initial experimental design was to synthesize monocationic complexes of Tc-99m that would, we hoped, mimic the known myocardial uptake of the monocationic species of Tl-201, Rb-81, Cs-129, and K-43 (*1,2*). Technetium-99m DMPE is our newest agent based on this rationale, and the resting distributions reported herein show useful properties despite the fact that they are not identical to those of Tl-201. Since an important property of any myocardial imaging agent is its ability to evaluate the functional reserve of the coronary artery under exercise conditions, studies designed to assess Tc-99m DMPE kinetics under variable hemodynamic conditions are under way. These studies should further clarify the potential clinical role of this new myocardial imaging agent.

FOOTNOTE

* The authors are grateful to Drs. Jim Benedict and John Lange of Proctor & Gamble Company for conducting this experiment.

ACKNOWLEDGMENTS

E.D. gratefully acknowledges support by the National Institutes of Health through Grant No. HL-21276.

REFERENCES

1. DEUTSCH E, GLAVEN KA, SODD VJ, et al: Cationic Tc-99m complexes as potential myocardial imaging agents. *J Nucl Med* 22:897-907, 1981
2. DEUTSCH E, BUSHONG W, GLAVEN KA, et al: Heart imaging with cationic complexes of technetium. *Science* 214:85-86, 1981
3. NISHIYAMA H, ADOLPH RJ, GABEL M, et al: Effect of coronary blood flow on thallium-201 uptake and washout. *Circulation* 65:534-542, 1982
4. COBB FR, BACHE RJ, GREENFIELD JC, JR.: Regional myocardial blood flow in awake dogs. *J Clin Invest* 53: 1618-1625, 1974
5. KLONER RA, GANOTE CE, JENNINGS RB: The "no-flow" phenomenon after temporary coronary occlusion in the dog. *J Clin Invest* 54:1496-1508, 1974
6. FISHBEIN MC, MEERBAUM S, RIT J, et al: Early phase acute myocardial infarct size quantification: validation of the triphenyl tetrazolium chloride tissue enzyme staining technique. *Am Heart J* 101:593-600, 1981
7. HAMILTON GW, TROBAUGH GB, RITCHIE JL, et al: Myocardial imaging with intravenously injected thallium-201 in patients with suspected coronary artery disease. *Am J Cardiol* 39:347-354, 1977
8. COOK DJ, BAILEY I, STRAUSS HW, et al: Thallium-201 for myocardial imaging: Appearance of the normal heart. *J Nucl Med* 17:583-589, 1976
9. CHERVU LR: Radiopharmaceuticals in cardiovascular nuclear medicine. *Semin Nucl Med* 9:241-256, 1979
10. STRAUSS HW, PITT B: Thallium-201 as a myocardial imaging agent. *Semin Nucl Med* 7:49-58, 1977
11. VAN DER VALL EE, HEIDENDAL GAK, DEN HOLLANDER W, et al: Metabolic myocardial imaging with I-123-labeled heptadecanoic acid in patients with angina pectoris. *Eur J Nucl Med* 6:391-396, 1981
12. KNAPP FF, AMBROSE KR, CALLAHAN AP, et al: Effects of chain length and tellurium position on the myocardial uptake of Te-123m fatty acids. *J Nucl Med* 22:988-993, 1981
13. NISHIYAMA H, SODD VJ, ADOLPH RJ, et al: Intercomparison of myocardial imaging agents: Tl-201, Cs-129, K-43 and Rb-81. *J Nucl Med* 17:880-889, 1976
14. ATKINS HL, BUDINGER TF, LEBOWITZ E, et al: Thallium-201 for medical use. Part 3: Human distribution and physical imaging properties. *J Nucl Med* 18:133-140, 1977
15. BROWN PH, KRISHNAMURTHY GT, BOBBA VVR, et al: Radiation dose calculation for Tc-99m HIDA in health and disease. *J Nucl Med* 22:177-183, 1981
16. CHERVU LR, NUNN AD, LOBERG MD: Radiopharmaceuticals for hepatobiliary imaging. *Semin Nucl Med* 12:5-17, 1982